Δελτίο της Ελληνικής Γεωλογικής Εταιρίας, τόμος L, σελ. 2210-2220
Πρακτικά 14ου Διεθνούς Συνεδρίου, Θεσσαλονίκη, Μάιος 2016

Bulletin of the Geological Society of Greece, vol. L, p. 2210-2220
Proceedings of the 14th International Congress, Thessaloniki, May 2016

GEOCHEMICAL MODELING FOR THE ASSESSMENT OF THE CO_2 STORAGE POTENTIAL IN THE MESOHELLENIC TROUGH, NW GREECE

Koukouzas N.[1], Kypritidou Z.[2], Purser G.[3], Rochelle C.A.[3] and Vasilatos C.[2]

[1]Centre for Research and Technology Hellas, Chemical Process and Energy Resources Institute, 15125, Maroussi, Greece, koukouzas@certh.gr

[2]Department of Economic Geology and Geochemistry, Faculty of Geology and Geoenvironment, National and Kapodistrian University of Athens, 15724, Athens, Greece, zach-kyp@geol.uoa.gr

[3]Environmental Science Center, British Geological Survey, Keyworth, NG12 5GG, Nottingham, England, gemm@bgs.ac.uk, caro@bgs.ac.uk

Abstract

Sandstone of the Pentalofos formation from the Mesohellenic Trough was examined as a potential reservoir for CO_2 sequestration. Experiments were carried out into batch reactors for 6 months by mixing a simplified porewater solution saturated with CO_2 (150 bar, 70°C) with crushed sandstone. The sandstone is mainly composed of carbonates, feldspars and quartz, and secondly of clays and phyllosilicates. Chemical analysis of aqueous samples showed an increase in the concentration of dissolved ions as the experiment progressed. Geochemical kinetic models that were constructed using the PHREEQC geochemical code showed that the fluid chemistry is controlled by carbonate and feldspar dissolution, clay and quartz precipitation and cation exchange reactions. The proposed models were also used to estimate the future changes in mineralogy of the sandstone in order to evaluate its suitability as a CO_2 reservoir.
Keywords: *sequestration, sandstone, PHREEQC, reservoir, dissolution.*

Περίληψη

Κονιοποιημένο ψαμμιτικό υλικό από το σχηματισμό Πενταλόφου της Μεσοελληνικής Αύλακας χρησιμοποιήθηκε σε πειράματα αυτοκλείστου όπου αντέδρασε με άλμη (0,5M NaCl) κορεσμένη με CO_2 (150 bar, 70 °C) για 6 μήνες. Το ψαμμιτικό υλικό αποτελείτο κυρίως από ανθρακικά, αστρίους και χαλαζία, με δευτερεύοντα αργιλικά και φυλλοπυριτικά. Οι χημικές αναλύσεις των ρευστών έδειξαν αύξηση των ιόντων, ενώ στο υλικό διαπιστώθηκαν αλλαγές στην αναλογία των φάσεων. Χρησιμοποιώντας το λογισμικό PHREEQC κατασκευάστηκε γεωχημικό κινητικό μοντέλο σύμφωνα με το οποίο οι κύριες αντιδράσεις που λαμβάνουν χώρα είναι η διάλυση των ανθρακικών και αστρίων, καθώς και η ιοντοανταλλαγή. Το μοντέλο χρησιμοποιήθηκε στην πρόβλεψη της πιθανής εξέλιξης του υδροφόρου σε βάθος χρόνου για την εκτίμηση της καταλληλότητας του πετρώματος ως αποθηκευτικός χώρος CO_2.
Λέξεις κλειδιά: *δέσμευση, ψαμμίτης, PHREEQC, ταμιευτήρας, διάλυση.*

1. Introduction

CO_2 capture and underground storage (CCS) has been proposed as a satisfactory method to reduce the atmospheric CO_2 concentrations, that play the key role in greenhouse phenomenon. Storage can be attained through injection into deep saline aquifers or gas depleted reservoirs. However the selection of the proper reservoir and its caprock is not trivial as CO_2 can cause a number of geochemical reactions that can affect their integrity and trapping potential. Some of them include the acidification of pore waters, dissolution of the primary minerals and precipitation of secondary, less stable, phases, changes in porosity and permeability of the whole (Black, *et al.*, 2015; Gaus, 2010).

A useful way to study geochemical processes, and water-rock reactions linked to CO_2 storage, is through geochemical modeling applied to the lithology encountered in the Mesohellenic Trough (MT) in NW Greece. The MT is a basin with a length of over 200 km and a width of 30-40 km in NW Greece. It is characterized as the largest and most important basin of the last orogenic stage (molasse basin) of the Hellenides (Figure 1).

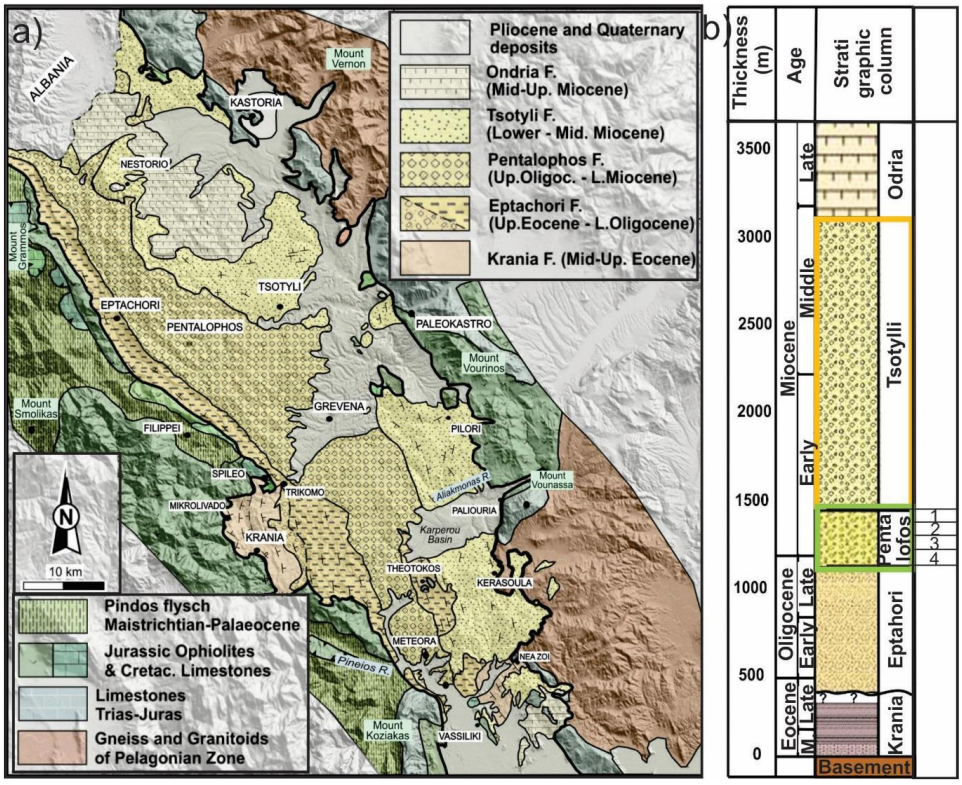

Figure 1 - Geological map (a) and stratigraphic column (b) of Mesohellenic trench (modified after Brunn (1956) and I.G.M.E. (1983) Tsotylli and Pentalofos Formations are highlighted - see text).

The sedimentary formations of the basin include deltaic conglomerates, alluvial scree, sandstones and clays of turbiditic and deltaic origin, floodplain and sandy shelf sediments, with a maximum thickness of 4 kilometers. The Tsotylli and Pentalofos Formations, correspond to local cap rock and reservoir respectively. The current work focuses on the Pentalofos Formation, with an age of Late Oligocene-Lower Miocene (25-23 Ma), which can be used as a reservoir due to its composition consisting mainly of loam and fine-grained sandstones (Vamvaka, 2009; Zelilidis *et al.*, 2002).

2. Materials and Methods

2.1. Materials

A sandstone sample from the Pentalofos Formation was used in batch reactor experiments. Quantitative mineralogical analysis of the sample before and after the reaction with CO_2 was attained by XRD analysis and data were processed using the Rietveld method.

2.2. Experimental set up and procedure

The sandstone sample was crushed and sieved to give 3 size fractions (<250, 250-500 and >500 μm). The 250-500 μm fraction was rinsed with acetone and filtered using a Buchner funnel containing a Whatman no.1 filter paper. 20g of this crushed and cleaned sandstone was mixed with 200ml of 0.5M NaCl solution (simplified porewater) inside the reaction vessel and heated in the oven to 70ºC. In order to ensure good rock-fluid mixing, it was stirred with a magnetic stirrer for 2 minutes every 4 hours (Figure 2). Periodic, rather than continuous, stirring ensured that the sandstone powder did not suffer too much mechanical abrasion.For the initial 37 days the sandstone and solution were allowed to partially equilibrate on CO_2-free conditions, with 15 bar of inert nitrogen in the headspace of the reaction vessel aiding sampling of the fluid. By day 37, the fluid had been sampled twice and addition of supercritical CO_2 (sCO_2) followed, which displaced the nitrogen initially present. CO_2 was maintained at a pressure of 150 bar for the rest of the experiment using a Teledyne ISCO 500D pump running in constant pressure mode. An additional number of 8 fluid samples were taken over this period. After a total duration of 184 days all the remaining aqueous solution that could be drained from the experiment was removed via a 'dip tube' that reached to the close to the bottom of the vessel, and its volume recorded. It was then slowly depressurised and dismantled to allow sandstone to be collected.

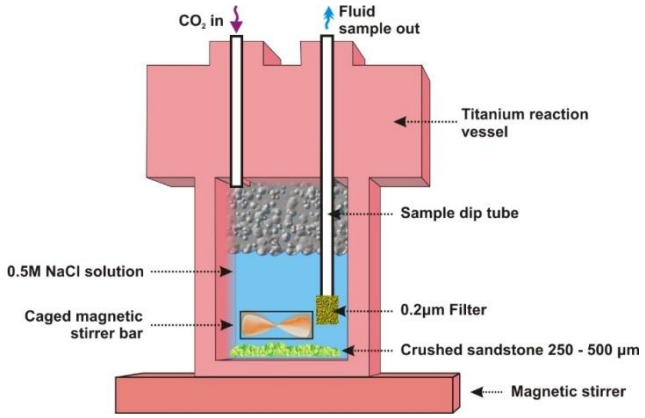

Figure 2 - Experimental arrangement for crushed sandstone sample.

2.3. Chemical Analysis

The experiment ran for approximately 6 months, during which a total of 10 fluid samples were collected. These were sub-sampled and prepared for analysis of pH, Eh (redox), anions, cations, alkalinity and iron (II) using the following methods. Most were pre-filtered through a 0.2 μm nylon Acrodisc filter. pH was measured at room temperature and pressure by an Orion bench top meter and glass pH probe calibrated using pH buffers of 4, 7 and 10 prior to sample analysis. The calibration of a Ag/AgCl Eh probe was checked using Zobell's solution prior to analysis of Eh. Alkalinity was measured using potentiometric titration as soon as practicable after sampling (usually within 1-3 days). The cation, anion and iron (II) samples were stored in a fridge at 4°C prior to analysis. Cations were analyzed using inductively coupled plasma mass spectrometry, anions by ion chromatography and reduced iron by UV-visible spectrophotometry.

2.4. Geochemical kinetic modelling

Geochemical models were constructed using the PHREEQC v.3.1 geochemical code with the llnl.dat database (Parkhust *et al.*, 1999). The parameters of reaction rates of each mineral were defined and solved by Ordinary Differential Equation (ODE) solver. The methodology followed is summarized in Figure 3. Speciation calculations were conducted on the basis of measured final solution composition for the base anions (Cl^-, HCO_3^-) and cations (Ca^{+2}, Mg^{+2}, Na^+, K^+, Al, Si, Fe_{total}). In each step, the data of previous calculations were used.

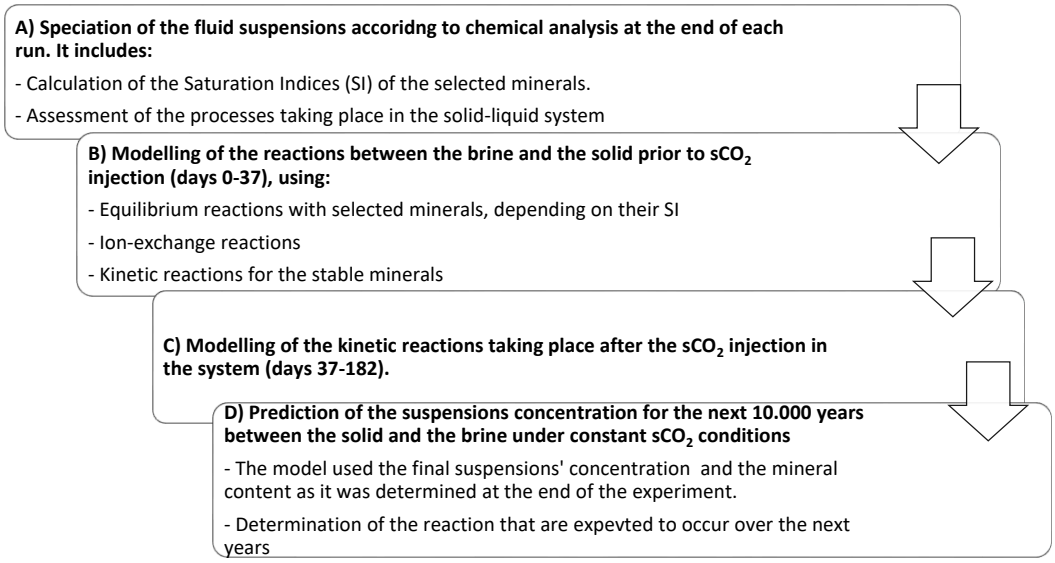

Figure 3 - Diagram showing the steps followed in constructing the geochemical models.

All simulations took into consideration the experimental conditions. The fugacity coefficient and solubility of the sCO_2 in 0.5M NaCl were calculated as 0.57 and 0.78 mol/kg H_2O respectively (Duan *et al.*, 2003). The reactive mineral mass was determined according to %wt mineral content of the sample and the solid/liquid ratio of 1:10. The effective diameter of the solid particles and their reactive surface area were calculated for the 250-500 μm particle size (assuming a spherical shape of the grains) and density of each mineral (Tester *et al.*, 1994). Reactive surface area (Equation 1) is the fraction of the mineral surface area that reacts with the solution and idealy is considered equal to the whole surface area.

Equation 1 – Reactive surface area

$$RS_A = \lambda n M S_A,$$

where n represents the number of moles and M the molar mass of the mineral respectively, and λ the reactive fraction (usually estimated experimentally). The values of λ were not measured, but defined to fit the models.

Reaction dissolution and precipitation rates were calculated using the Transition State Theory (TST) (Equations 2 and 3). Both dissolution (r_d) and precipitation (r_p) reactions are subject to the system temperature and pH which influence the reaction constants (Arrhenius Law), separating an acid, neutral and base part respectively.

Equation 2 – Dissolution rate kinetics (Lasaga, 1984)

$$r_d = RS_A * \left(k_0^{nu} \exp\left[\frac{-E_a}{R}\left(\frac{1}{T} - \frac{1}{298.15}\right)\right] + k_0^{acid} \exp\left[\frac{-E_a}{R}\left(\frac{1}{T} - \frac{1}{298.15}\right)\right] a_H^{acid} + k_0^{base}\left[\frac{-E_a}{R}\left(\frac{1}{T} - \frac{1}{298.15}\right)\right] a_{OH}^{base}\right) * \left|1 - \Omega_n^p\right|^q ,$$

where k_0 is the rate constant at 25 °C (mol m^{-2} s^{-1}), Ea the activation energy (J mol^{-1}), a_i the activity of ion i, R the gas constant (8.314 J mol^{-1} K^{-1}) and T the absolute temperature (K). Ω is the mineral saturation index and p,q are constants.

Equation 3 – Precipitation rate kinetics (Van Pham *et al.*, 2011)

$$r_p = -(k_{pre} + k_{add}) * RSA * \left|\Omega_n^p - 1\right|^q - k_N \exp\left[-\Gamma_{ij}\left(\frac{1}{\sqrt[3]{T^2}\ln\Omega}\right)^2\right],$$

where k_{pre} and k_N are the precipitation and nucleation constants respectively (mol m^{-2} s^{-1}), Γ_{ij} the nucleation constant and k_{add} the influence of additional mechanisms, such as carbonates or hydroxyl ions (Hellevang *et al.*, 2013). Kinetic dissolution and precipitation kinetic parameters were taken from Palandri and Kharaka (2004), Marty *et al*. (2015) and Van Pham *et al.* (2011).

3. Results

3.1. Sandstone mineralogy

The mineralogy of the samples before and after the interaction with sCO_2-brine was determined through XRD analysis. The bulk sample are consisted mainly of calcite (38.2%), quartz (20.9%), albite (14.9%) and orthoclase (10.2%). Secondary phases include dolomite (4.5%), clinochlore (8.2%) and montmorillonite (2.8%). Kaolinite (0.2%) and muscovite (0.1%) are of little importance. After the reaction with sCO_2, new phases were not formed, instead there was a mass transfer among the pre-existing mineral phases. More specifically, albite, orthoclase, clinochlore, calcite and dolomite dissolved to 12.7%, 9.9%, 34.8% and 2.1% respectively. The dissolution led to precipitation of clay minerals and silica (in the form of quartz) increasing their percentages to 0.7% for kaolinite, 3.6% for montmorillonite and 27.7% for quartz. Using the initial mineral contents of the sample, the specific surface was calculated for each mineral (Table 1).

Table 1 - Mineral parameters for the kinetic modelling.

Mineral phase	m (moles/kg H_2O)	ρ (g/cm^3)	S_A (m^2/g)
Albite	0.0566	2.62	6.35E-03
Orthoclase	0.0366	2.56	6.50E-03
Calcite	0.3817	2.71	6.14E-03
Dolomite	0.0244	2.65	6.28E-03
Montmorillonite	0.0051	2.35	7.08E-03
Kaolinite	0.0008	2.60	6.40E-03
Muscovite	0.0003	2.82	5.90E-03
Chlorite	0.0138	2.65	6.28E-03
Quartz	0.3479	2.62	6.35E-03

Ion exchange capacity was calculated by the CEC (meq/100g) reported in literature for each mineral and their relative mass. The calculated CEC ranges from 2.5 to 6 meq/100g. The average value used is 4.31 meq/100g resulting to 0.0008 moles per 20g of solid.

3.2. Fluid chemistry

The initial brine concentration, as well as the suspensions' composition prior to and after the sCO_2 injection were determined. sCO_2 injection increases calcium, magnesium and bicarbonate concentrations, (which are most likely caused by calcite and dolomite dissolution) and the solution pH decreases. K and Na are well correlated with silica, which suggests feldspar dissolution (Figure 4).

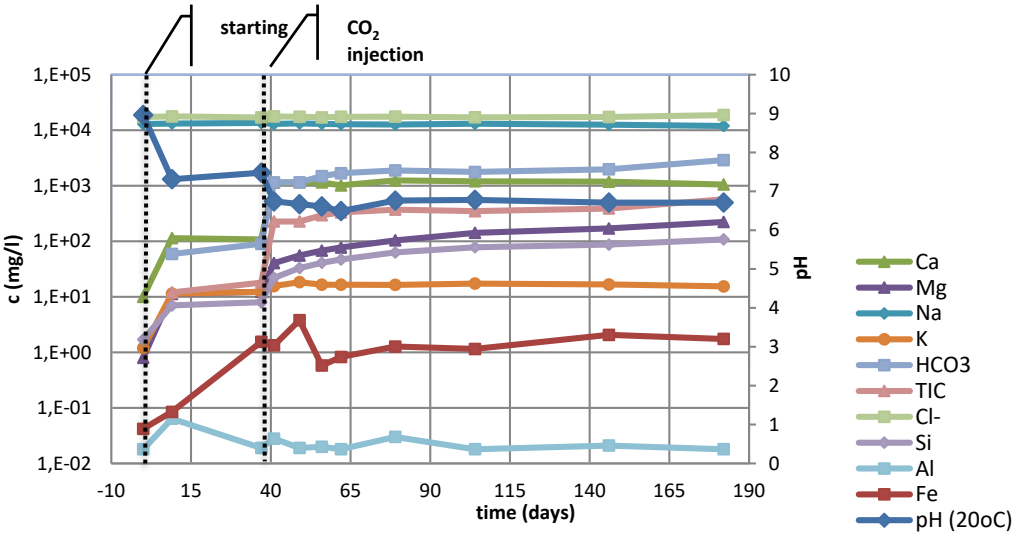

Figure 3 - Evolution of fluid chemistry as a function of time during the 6 months of the experiment (Purser *et al.*, 2015).

3.3. Geochemical modelling

3.3.1. Fluid speciation

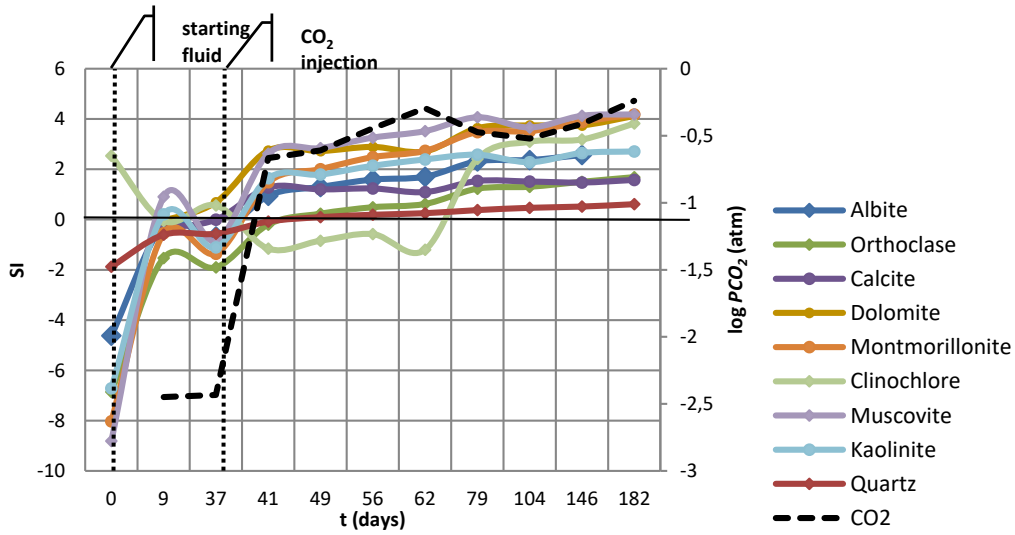

Figure 4 - Saturation indices (SI) for the mineral phases of the sandstone sample.

Geochemical modelling involved using the measured fluid compositions and calculating mineral saturation indices (Figure 5). The brine was undersaturated with respect to most minerals (SI<0) prior to sCO_2 injection, and saturated with respect to calcite (SI=0). After the addition of CO_2, many phases were oversaturated (SI>0).

3.3.2. Equilibrium modelling

Equilibrium calculations for brine-rock interaction were based on the experimental data at 37, i.e. before addition of CO_2.

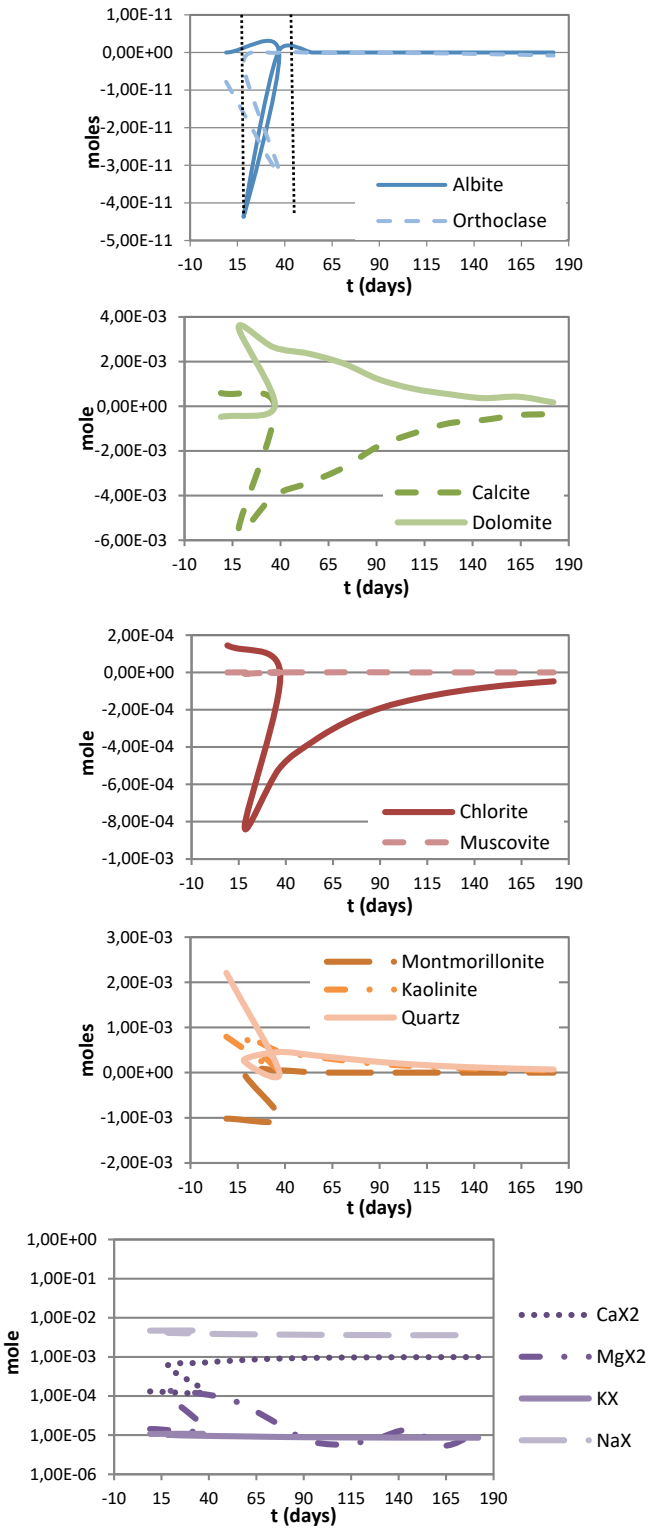

Figure 5 - Mole transfer prior to (equilibrium) and after (kinetics) the sCO_2 injection as a function with time from the beginning to the end of the experiment.

Whilst we recognise that this is a relatively short period of reaction time, it is informative to undertake these calculations to ascertain which reactions may have neared steady state conditions. The model used primarily equilibrium and cation exchange reactions. Taking into account the above speciation calculations, calcite, albite, dolomite, clinochlore were considered at equilibrium with the initial fluid and ion-exchange was attributed to surface sites occupied by Ca.

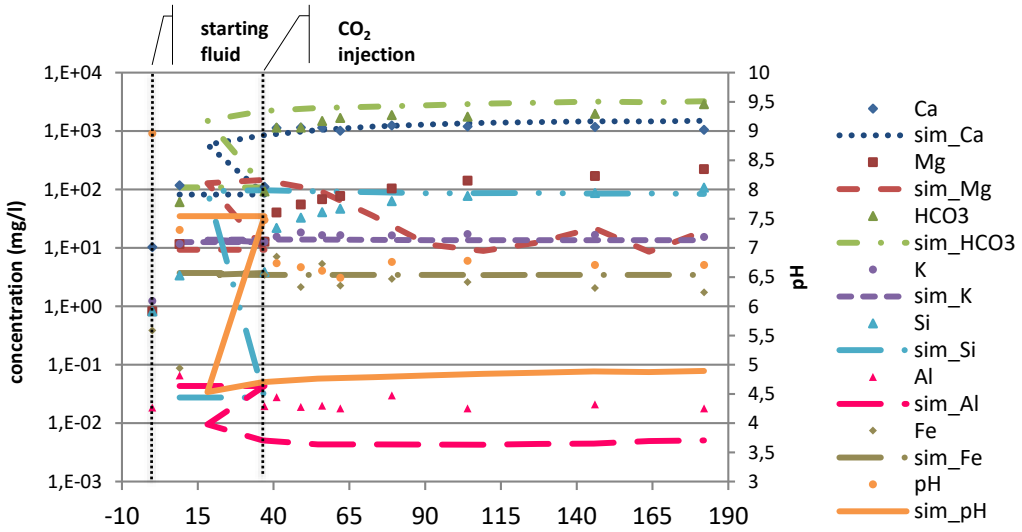

Figure 6 - Modelled and experimental suspensions composition as a function of time from the start (equilibrium reactions) to the end (kinetic reaction) of the experiment.

3.3.3. Kinetic model

A kinetic model was constructed based on the above equilibrium observations and fluid chemical changes between injection of CO_2 and the end of the experiment. According to the calculated SIs at the speciation, no equilibrium occurs after the sCO_2 injection. The kinetic modelling consists of kinetic reactions and ion-exchange. All input data were kept constant, except the reaction mineral mass which was adjusted to the equilibrium model results.

The simulated liquid is slightly acidic in respect to the experimental pH (Figure 7). The experimental pH measurement was of the degassed fluid that was extracted from the experiment, so its value is expected to be higher than the pH calculated by the model. Generally, the experimental data fit very well to the model results, with minor deviations. It must be noted that the constant suspension sampling during the experiment results in changing the solid/liquid ratio resulting in condensation.

The kinetic simulations show that albite, muscovite and orthoclase undergo limited dissolution (Figure 6). Silicates dissolution is followed by the precipitation primarily of kaolinite, montmorillonite and secondary silica (expressed as “quartz” in the model). Calcite, which was precipitating before CO_2, dissolve after the injection. Dolomite precipitates in contrast to the experimental data. Na and K are released from the surface sites, and are replaced by Ca and Mg.

3.3.4. Prediction model

The prediction model used the concentration of the final suspension sampled and the mineral mass determined by the XRD analysis for the solid after the reaction with sCO_2. Kinetic constants remained unchanged. The mineral evolution was simulated over a 10.000 year timescale. We recognise that this is extending an experimentally-derived model far in excess of its validated time period, and the results should be seen as tentative. However, this is a useful exercise as it helps identify the possible long-term fate of stored CO_2 and its impact on the host lithologies.

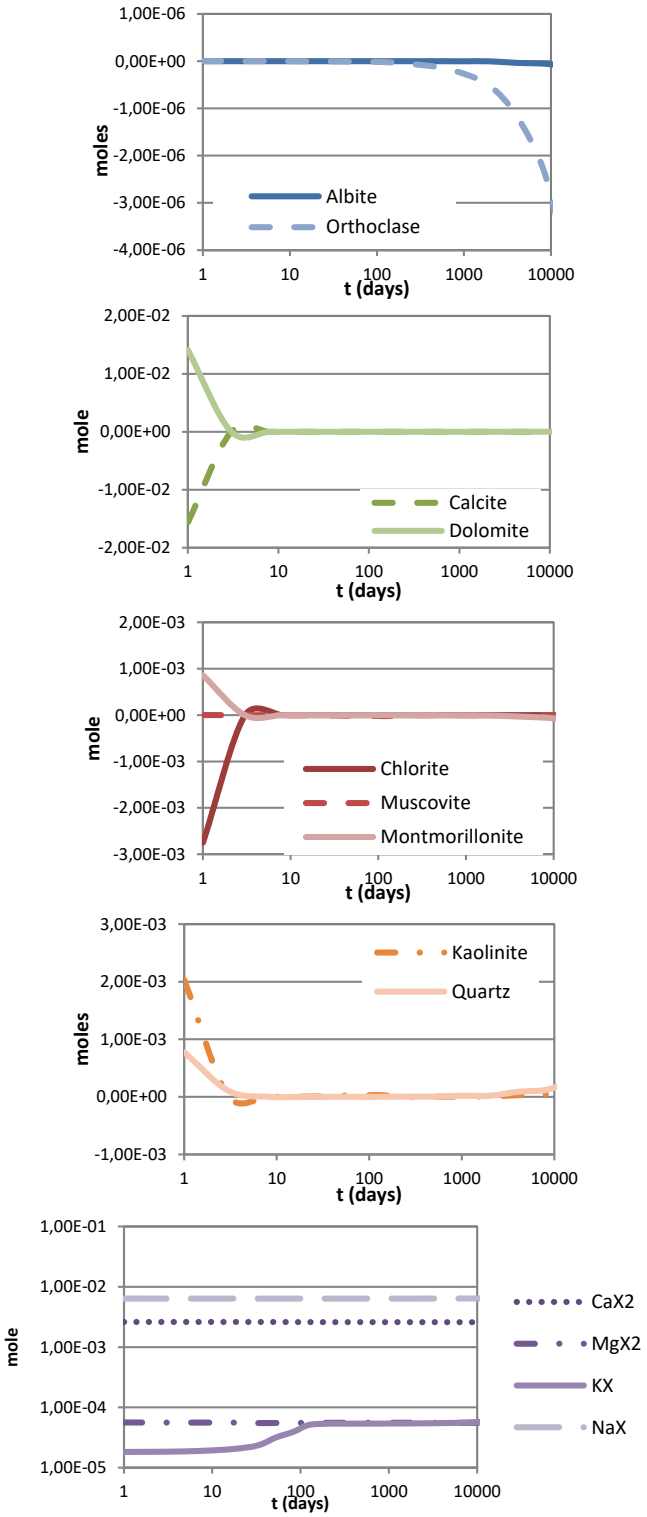

Figure 7 - Predictions of mineral evolution with the sandstone.

Albite remains unreactive. Chlorite and muscovite react for 10 years, then chlorite is being exhausted, and muscovite reacts again after 7000 years. Orthoclase is reactive till the end of the simulation.

Silicates dissolution result in precipitation primarily of montmorillonite and quartz, and secondly of kaolinite. Dolomite precipitates and calcite dissolves for 10 years, until it is exhausted. Then dolomite begins to dissolve. Generally, the phases of the solid seem to reach equilibrium after 10 years of reaction with sCO_2 (except orthoclase) leading to stabilization of the sandstone mineralogy (Figure 8).

4. Conclusion

The kinetic model, which was proposed to simulate the rock-brine interactions with sCO_2, showed that the fluid and sandstone chemistry is controlled primarily by the carbonates and secondly by the clinochlore and muscovite dissolution. The dissolution of feldspars is of less importance. These reactions are expected to continue for another 10 years (except orthoclase dissolution), after which the system tends towards equilibrium.

The above suggested models are based on a number of uncertainties. Surface area and ion-exchange were not measured but rather they were estimated using reference data Moreover, the ideal chemical compositions of the mineral phases were used instead of the real ones, especially in the case of chlorite and montmorillonite. The knowledge of the exact mineral stoichiometry would have given more accurate results regarding the fluids' chemistry. Despite these uncertainties, the proposed model provides a first estimation of the geochemical reactions occurring between the sandstone and a CO_2-saturated brine, helping in its evaluation as a potential CO_2 reservoir.

5. Acknowledgments

This research has been co-financed by the European Union (European Social Fund - ESF) and Greek national funds through the Operational Program "Education and Lifelong Learning" of the National Strategic Reference Framework (NSRF) - Research Funding Program: Thales. Investing in knowledge society through the European Social Fund. The authors would also specifically like to thank all the staff of the British Geological Survey (BGS) that were involved in the batch experiments on samples of Greek sandstone, limestone and borehole cement and that contributed to the sample preparation and provided the fluid analysis results. Special thanks should also be given to Alexandros Tasianas and Nikolas Tsoukalas from CERTH for their contribution in redacting this paper, as well as the National and Kapodestrian University of Athens for its support in this work. GP publish with the permission of the Executive Director of the British geological Survey, NERC.

6. References

Black, J.R., Caroll, S.A. and Haese, R.R., 2015. Rates of mineral dissolution under CO2 storage conditions, *Chemical Geology*,399, 134-144.

Brunn, J., 1956. Contribution a l' étude geologique du Pinde serpentrional et d' une partie de la Macedoine occidentale, *Annales Géologique des Pays Hellénique,* 7, 1-346.

Duan, Z. and Sun, R., 2003. An imroved model calculating CO2 solubility in pure water and aqueous NaCl solutions from 273 to 533 K and from 0 to 2000 bar, *Chemical Geology*, 193, 257-271.

Gaus, I., 2010. Role and impact of CO2-rock interactions during CO2 storage in sedimentary rocks, (Review), *International Journal of Greenhouse Gas Control*, 4, 73-89.

Hellevang, H., Pham, V.T. and Aaagaard, P., 2013. Kinetic modelling of CO2-water-rock interactions, *International Journal og Greenhouse Gas Control*, 15, 3-15.

I.G.M.E. (Institute of Geology and Mineral Exploration), 1983. Geological Map of Greece, Redaction from: Bornovas, J. and Rondogianni-Tsiambaou, Th., s.l.s.n.

Lasaga, A., 1984. Chemical kinetics of water-rock interactions, *Journal of Geophysical Research*, 89, 4009-4025.

Marty, N.C.M., *Claret, F., Giffaut, E., Madé, B. and Tournassat, C.,* 2015. A database of siddolution and precipitation rates for clay-rocks minerals, *Applied Geochemistry*, 55, 108-118.

Palandri, J. and Kharaka, Y., 2004. A compilation of rate parameters of water-mineral interaction kinetics for application to geochemical modeling, Mento Park, California: U.S. Geological Survey.

Parkhust, D. and Appelo, C., 1999. User's guide to PHREEQC (Version 2) - A computer program for speciation, batch-reaction, one-dimensionla transport, and inverse geochemical calculations, s.l.: U.S. Geologcal Survey-Resources Investigations, Report 99-4259, 310.

Purser, G. and Rochelle, C., 2015. A brief note describing batch experiments on samples of Greek sandstone, limestone and borehole cement., s.l.: British Geological Survey Commercial Report, CR/15/035, 22 pp.

Soave, G., 1972. Equilibrium constants from modified Redlich-Kwong equation of state, *Chemical Engineering Science*, 1197-1203.

Tester, J.W., Worley, W.G., Robinson, B.A., Grigsby, C.O. and Feerer, J.L., 1994. Correlating quartz dissolution kinetics in pure water from 25 to 625oC, *Geochemica et Cosmochimica Acta*, 58(11), 2407-2420.

Vamvaka, A., 2009. Geometry of deformation and kinematic analysis in Mesohellenic Trough, s.l., PhD Thesis, Aristotle University of Thessaloniki, Department of Geology.

Van Pham, T., Lu, P., Aagaard, P., Zhu, C. and Hellevang, H., 2011. On the potential of CO2-water-rock interactions for CO2 storage using a modified kinetic model, *International Journal of Greenhous Gas Control*, 5, 1002-1015.

Zelilidis, A., Piper, D. and Kontopoulos, N., 2002. Sedimentation and basin evolution of the Oligocene-Miocene Mesohellenic basin, Greece, *AAPG Bulletin*, 86(1), 161-182.